Kua and Tan *Biochar (2023)5:36*
https://doi.org/10.1007/s42773-023-00234-w

Biochar

ORIGINAL RESEARCH

Open Access

Novel typology of accelerated carbonation curing: using dry and pre-soaked biochar to tune carbon capture and mechanical properties of cementitious mortar

H. W. Kua[1*] and S. M. H. Tan[1]

Abstract

One of the challenges of promoting accelerated carbonation curing (ACC) of concrete as a carbon sequestration strategy is ensuring that carbonation will not deteriorate mechanical strength. This study examined the mechanical strength, water sorptivity and carbonation efficiency of ten types of mortar containing dry or pre-soaked biochar subjected to internal and/or external carbonation. The results obtained enabled a typology of ACC to be proposed, in which the carbon dioxide absorption of mortar containing various types of CO_2-dosed biochar ranged between 0.022% and 0.068% per unit dosage hour. In particular, the mortar containing dry biochar dosed with carbon dioxide was the top candidate for concurrently increasing both compressive strength (54.9 MPa) and carbon dioxide absorption (0.055% per unit dosage hour). Mortar containing pre-soaked biochar dosed with carbon dioxide was identified as a strategy that achieved the highest carbonation efficiency (0.068% per unit dosage hour), but it also reduced compressive strength (45.1 MPa). Collectively, the proposed typology offers a useful overview of the different ways by which biochar can be used to tune ACC in mortar, according to any technical constraints and/or intended functions of the carbonated concrete components.

Highlights

- A typology of accelerated carbonation curing for mortar was proposed
- Dry and pre-soaked biochar was subjected to internal and/or external carbonation
- Compressive and flexural strength, water sorptivity, and carbonation efficiency were measured
- Dry biochar subjected to internal carbonation increased strength and carbonation of mortar

Keywords Biochar, Pre-soaked, Carbonation effectiveness, Carbonation efficiency, Accelerated carbonation curing

Handling editor: Wenfu Chen

*Correspondence:
H. W. Kua
bdgkuahw@nus.edu.sg
Full list of author information is available at the end of the article

Graphical Abstract

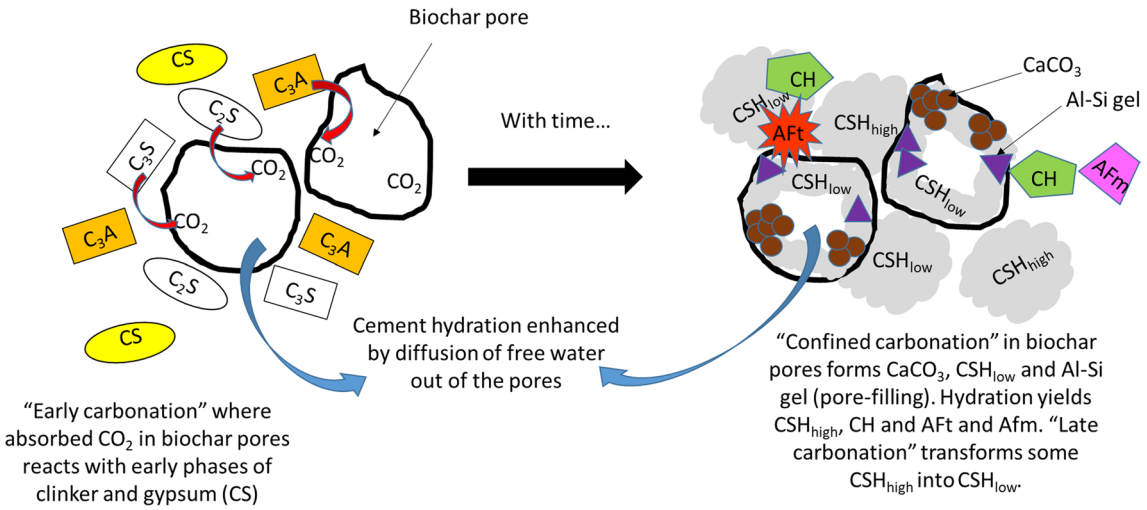

1 Introduction

In recent years, a relatively simple and effective method of capturing and sequestering carbon dioxide (CO_2) in concrete by mineralization has been widely discussed in the literature; this is now known as Accelerated Carbonation Curing (ACC), which is a process whereby cementitious materials are exposed to the injected CO_2 that reacts with its unhydrated components (Kashef-Haghighi et al. 2015), resulting in the conversion of the absorbed CO_2 into various forms of stable carbonates (Rostami et al. 2012). This method is preferred to natural, or weathering, carbonation because natural diffusion of atmospheric CO_2 through the pores in concrete or mortar is very slow (Gupta et al. 2017). In contrast, ACC accelerates the carbonation rate and increases the net amount of CO_2 sequestered (Lim et al. 2019); furthermore, the conditions of the ACC process can be adjusted in a controlled environment (usually a carbonation chamber) (Liu and Meng 2021). For ACC to be a commercially viable technology, it is important to understand the effects of ACC on the mechanical properties and permeability of the mortar or concrete (Tan and Sia 2009).

Studies on the use of biochar in concrete are a relatively new field. Many studies have shown how the hygromechanical properties of concrete/mortar can be significantly enhanced by incorporating biochar into the mix (for example, Choi et al. 2012; Ahmad et al. 2015; Ferro and Restuccia 2016; Gupta and Kua 2017, 2019). On the other hand, there are currently only a few studies on the use of biochar to enhance ACC. ACC should not be seen as a method with a singular goal of capturing carbon; in this light, these studies provided insights into how biochar can be used to modify the carbon absorption capacity and mechanical properties of concrete. Hence, the aim of this study is to propose a typology of ACC for cementitious mortar, using biochar as means of tuning the mortar's carbon capture and mechanical properties. The objectives are to quantify and compare the compressive strength, flexural strength, water sorptivity and CO_2 adsorption of various types of cementitious mortar containing two types of biochar—dry and pre-soaked biochar—subjected to two different carbonation methods (internal and external).

2 Literature review

2.1 Contribution of biochar to carbon sequestration potential of mortar under accelerated carbonation curing

The CO_2 adsorption capacities of different types of biochar is well documented in the literature. It's carbon sequestration capability is dependent on its physical properties, such as pore volume and specific surface area (Gupta and Kua 2017; Dissanayake et al. 2020). Table 1 presents an overview of some of the key studies on various types of unmodified biochar in room temperatures of 23–30 °C. As shown in Table 1, under room temperature, unmodified biochar is capable of capturing between 0.45 and 1.67 mmol of CO_2 per gram of biochar (that is, between 19.8 and 73.5 mg CO_2 per gram of biochar). A comprehensive compilation of the CO_2 adsorption capacity of modified biochar was

Table 1 Summary of key studies on the CO_2 adsorption capacity of unmodified biochar

Feedstock type	Pyrolysis temperature (°C)	Specific surface area (BET) ($m^2\ g^{-1}$)	Total pore volume ($cm^3\ g^{-1}$)	Adsorption temperature °C	Maximum CO_2 absorption capacity (mmol g^{-1})	References
Soybean straw	500	0.04	Not reported	30	1.02	Zhang and Shao (2016)
Hickory wood	300	0.10	Not reported	25	0.78	Creamer et al. (2014)
Sugar cane bagasse	300	5.20	Not reported	25	0.88	
Sewage sludge	500	10.12	0.022	25	0.47	Xu et al. (2016)
Pig manure	500	31.57	0.044	25	0.53	
Wheat straw	500	20.20	0.041	25	0.78	
Sawdust	450	8.76	Not reported	30	0.45	Madzaki and KarimGhani (2016)
Mixed wood sawdust	300	0.83	0.123	28	1.67	Gupta et al. (2017); Gupta et al. (2018b)
Processed peanut	500	2.15	0.00655	23	0.86	Gupta et al. (2021)
Mixed wood sawdust	400	126.88	0.104	28	1.30	Gupta (2021)

presented by Dissanayake et al. (2020), which ranges from 15 to 99 mg CO_2 per gram of biochar.

The literature on ACC of concrete is also well developed. For example, Suescum-Morales et al. (2021) found that the CO_2 adsorption of concrete mixes containing different proportions of natural and recycled aggregates was approximately between 24 and 27 kg CO_2 per ton of concrete mix, which is approximately 13–14.4% of the mass of cement. Rostami et al. (2012) reported that the carbonation of cement paste for only 2 h at early stage (18 h from mixing) could sequester 11.50 kg of CO_2 for every 100 kg of cement (that is, 11.5% of the mass of cement). Shao et al (2014) found that concrete containing grounded limestone adsorbed CO_2 at 17.44% of mass of cement. On the other hand, adding biochar saturated with CO_2 (also known as internal carbonation) into mortar at 2–10% by mass of cement can only account for additional adsorption capacity of about 0.2–0.99% of cement mass, which is negligible (Gupta et al. 2018a, b, c). The true significance of biochar to the overall carbon sequestration or reduction in mortar can be understood by accounting for the difference in the net life cycle carbon emission of biochar and the materials it partially replaces in mortar—that is, cement (Muthukrishnan et al. 2019; Gupta et al. 2020; Gupta and Kua 2020) or sand (Praneeth et al. 2021; Maljaee et al. 2021). Roberts et al. (2010) estimated that the average net (life cycle) greenhouse gas emissions from the *biochar system* made from stover and yard waste are − 864 and − 885 kg CO_2-e emissions per tonne dry feedstock (or, about 300 kg of biochar), respectively; this implies that replacing 1 kg of cement with 1 kg of biochar can potentially reduce the net emission by 3.65 kg CO_2-e. That is, the real carbon-reducing value of using biochar must be appreciated in a life cycle systemic context. Furthermore, what is more important is the net effect that ACC has on the mechanical properties of mortar.

2.2 Impact of ACC on mechanical properties of mortar

There are different carbonation pathways in concrete (Teir et al. 2005). Clinker contains predominantly tricalcium silicate (alite, C_3S) and the polymorph beta-dicalcium silicate (belite, β-C_2S), which are the most hydraulically reactive calcium silicate minerals—that is, they participate actively in the cement hydration process. During clinker production, when the product was cooled at a rate lower than about 500°C min^{-1}, some of the β-C_2S can transform into another polymorph known as gamma-dicalcium silicate (belite, γ-C_2S). Although chemical impurities (such as Na_2O, P_2O_5, B_2O_3, Cr_2O_3 and K_2O) are known to stabilize the β-C_2S, if their respective concentrations fall below approximately 1.2%, 0.3%, 0.3%, 1.0% and 1.5% (Zhao 2012), traces of γ-C_2S can still be present in the clinker. Although γ-C_2S is non-hydraulic and has no hydration reactivity, C_3S, β-C_2S, and γ-C_2S were found to be almost equally reactive to carbonation at near room temperatures (Ashraf and Olek 2016). In the early stage of carbonation, C_3S and β-C_2S were involved in the combined action of hydration and carbonation as follows:

$$10(3CaO \cdot SiO_2) + 23CO_2 + 6H_2O \rightarrow 7CaO.10SiO_2 \cdot 6H_2O + 23CaCO_3 \quad (1)$$

$$10(2CaO \cdot SiO_2) + 16CO_2 + 3.5H_2O \rightarrow 4CaO.10SiO_2 \cdot 3.5H_2O + 16CaCO_3 \quad (2)$$

By-products of hydration, such as calcium hydroxide (CH), calcium silicate hydrate (CSH) and calcium aluminate hydrate (CAH), under further carbonation (Kaliyavaradhan and Ling 2017):

$$Ca(OH)_2 + CO_2 \rightarrow CaCO_3 + H_2O \quad (3)$$

$$(CaO)_x(SiO)_y(H_2O)_z + xCO_2 \rightarrow xCaCO3 + y(SiO_2).(H_2O)_t + (z - yt)\,H_2O \quad (4)$$

$$4CaO.Al_2O_3.13H_2O + 4CO_2 \rightarrow 4CaCO_3 + 2Al(OH)_3 + 10H_2O \quad (5)$$

The carbonation of CSH binder gel (Eq. (4)) is a complex decalcification–polymerization process in which the CSH gel is decalcified and the liberated lime (CaO) molecules can react with the carbonate ions to form $CaCO_3$ (Lagerblad 2005).

On the other hand, non-hydraulic γ-C_2S carbonates by a different mechanism that can be summarized as follows:

$$CO_2 + H_2O \rightarrow H_2CO_3 \quad (6)$$

$$2CaO.SiO_2 + 2H_2CO_3 \rightarrow CaCO_3 + SiO_2 + 2H_2O \quad (7)$$

That is, CO_2 first dissolves in water to yield H_2CO_3 solution, and the latter ionizes into H^+, HCO_3^- and CO_3^{2-}. The leaching of Ca^{2+} from γ-C_2S occurs in an exothermic reaction, with the gel on the surface of the calcium silicate particles dissolved, releasing Ca^{2+} and SiO^{-4} ions (Wang et al. 2022; Maries 1985).

The $CaCO_3$ particles formed are finer than those of ordinary portland cement and so the presence of $CaCO_3$ results in better packing of particles between cement and $CaCO_3$ (You et al. 2014; Ali et al. 2015). This densification of the cement matrix accelerates cement hydration as water retention is improved, which in turn accelerates concrete hardening and improves early-age strength of concrete (Matschei et al. 2007; Ali et al. 2015; Cao et al. 2019). Rostami et al. (2012) investigated the effect of ACC on the compressive strength development of plain cement mortar, which was carried out for 18 h from mixing for a duration of 2 h; after 28 days, they reported an improvement of 30% in compressive strength compared to control paste that underwent air curing. However, prolonged exposure to CO_2 has been reported to lower the compressive strength of both cement mortar. For example, Junior et al. (2014) reported that while carbonation curing for 1 and 2 h resulted in an improved compressive strength of cement mortar, carbonation curing for 2 h and more (up to 12 h) led to a reduction in compressive strength. The reason is that despite the increase in $CaCO_3$ formed, the excessive consumption of water in the pores of mortar interrupts hydration essential for strength development (Papadakis 2000). Furthermore, prolonged carbonation can lead to the decalcification of CH (Eq. 3) or CSH binder gel (Eq. 4) thus reducing the binding capacity in the cementitious matrix and causing a loss in its structural integrity (Li et al. 2019, 2017). In summary, these studies indicate the presence of a "tipping point" in carbon adsorption over which mechanical properties of the mortar will be compromised.

Similarly, prolonged exposure to CO_2 has also been reported to increase the initial water absorption of plain cement mortar and biochar-mortar. For example, Gupta et al. (2021) found that after 28 days, the total water absorption of both carbonated plain mortar and biochar-mortar are higher than that of their water-cured counterparts and this increase is mainly contributed by higher initial water sorptivity. Moisture stored in capillary pores of cement matrix facilitates hydration, which aids in pore structure refinement through the generation of hydration products (Gupta et al. 2021); however, ACC results in water consumption in these fine capillary pores for carbonation and this reduces the degree of hydration, which leads to higher porosity and initial water sorptivity of the cementitious matrix (Yang and Wang 2021).

The application of biochar to aid ACC is a relatively new approach. A better understanding of the combined effects of internal and external carbonation, and internal hydration, afforded by biochar particles is crucial to evaluate the potential of ACC with biochar mortar.

2.3 Internal curing and internal carbonation

A fundamental concept explored in this work is the internal curing effect of biochar in mortar. When excess water during mixing is not absorbed by cement mortar, water is lost through evaporation or concrete bleeding. This results in the formation of capillary pores and air voids (Kim et al. 2019), thus reducing the mechanical strength and increasing the water sorptivity of cement mortar (Gupta et al. 2017 and Gupta et al. 2018a). In the presence of biochar, its pores absorb and retain excess moisture in the matrix, and the moist pore surfaces act as nucleation spots that facilitate development of hydration products (Gupta et al. 2018b). These products fill the pores and densifies surrounding matrix, contributing to its strength and water-tightness development. The internal effect manifests when a humidity gradient occurs between the water-logged biochar and its surrounding cementitious matrix, which results in the water desorbing

from the pores (Gupta and Kua 2018). Hydration products formed from this release of additional moisture from biochar offsets the empty pore spaces of the cementitious matrix during the hardening phase, resulting in a more continuous and uniform microstructure (Mrad and Chehab 2019). Specifically, Gupta and Kua (2018) discovered that the addition of pre-soaked biochar reduced water accessible porosity by 18–20% and the depth of water penetration by 55–60%. Significant improvement in mechanical properties were also observed when pre-soaked biochar was used compared to addition of dry biochar in mortar.

The first ever study on the hygromechanical effect of internal carbonation by biochar was done by Gupta et al. (2018a). The adsorbed CO_2 in the biochar pores set off carbonation in the biochar pores and at the interfacial transition zone between the biochar and the cementitious matrix, hence degrading the CH and CSH in these areas. This gave rise to micro-cracks and air voids that weakened the mortar microstructure. However, this result would only occur when the magnitude of the negative effect of the aforementioned air void formation outstripped the positive effects of hydration product formation on strength development. Gupta (2021) is the first to study the effects of using CO_2-saturated biochar in mortar mix. He found that cement hydration is less affected in internally carbonated pastes compared to external carbonation in 28-day age cement paste samples, which was shown in 8–10% higher compressive strength.

2.4 Knowledge gaps, novelty and contribution to knowledge

Most of the works reviewed in this study involved exposing the mortar or concrete samples to CO_2 dosage only after pre-carbonation conditioning in which they were moist cured in-mold. Most studies involving biochar evaluated the effects of either internal carbonation or external carbonation on the durability and mechanical properties of cement mortar. When external and internal carbonation were compared [for example, Gupta (2021)], only dry biochar was used. Pre-carbonation conditioning delayed the start of the ACC and it is important to know how much this delay will reduce the overall carbon absorption by, compared to if in-mold samples were dosed with CO_2 immediately after casting; this was done in this study. We also investigated the combined effects of internal and external carbonation on the durability and mechanical properties of cement mortar, and include both dry and pre-soaked biochar in the mortar samples.

It is important to look at internal carbonation in carbonating dry and pre-soaked biochar for several reasons. Firstly, CO_2 that is already present on the carriers—in our case, biochar particles—before mixing in the mortar will initiate carbonation processes mainly represented by Eqs. (1)–(2) (herein termed as "early carbonation"). Few studies have examined the effects of the interactions among the products of such "early carbonation", those from carbonation that occurs later [herein termed as "late carbonation" and it is described mainly by Eqs. (4)–(5)] and hydration. Secondly, biochar enhances properties of cementitious materials by modifying the flow and distribution of free water in the mix to enhance internal curing in mortar samples (Gupta and Kua 2018). Internal curing by dry and pre-soaked biochar has different effects. By mixing CO_2 with dry and pre-soaked biochar, we can understand how this different nature of internal curing, caused by different ways of distributing water by the dry and pre-soaked biochar, can affect the aforementioned interactions between carbonation and hydration in biochar mortar. Thirdly, when dry biochar dosed with CO_2 is subjected to "early carbonation", the products are confined in and around the pores, and carbonation is confined (herein called "confined carbonation"). It is important to understand how the different physical, chemical and mechanical properties of mortar will be affected. Finally, it will be important to explore how more conventional ways of ACC can possibly be augmented using CO_2-dosed dry and pre-soaked biochar, in terms of compressive strength, flexural strength, water sorptivity, $CaCO_3$ and CH contents, and microstructure development. It is hoped that the results can help to provide a scientific basis for creating a typology of ACC methods, using biochar as a tuning agent.

3 Materials and methods

3.1 Preparation of dry and pre-soaked biochar; CO_2-dosing of biochar and mortar samples

The biochar used in this study was produced by the pyrolysis of an assortment of wood from Thailand (including teak, eucalyptus, mango and durian), at a temperature range from 300 °C to 500 °C. The biochar was delivered in a coarse form, and it was ground and then sieved using a 0.5-mm stainless steel mesh screen. The biochar was found to have a Specific Surface Area (BET) of 0.066 m^2g^{-1}, and Total Pore Volume of 0.050 cm^3g^{-1}. Prior to mixing it in the mortar samples, the biochar was preheated at 200℃ at a heating rate of 5 °Cmin^{-1} and subjected to a residence time of 1 h to remove impurities such as volatile organic matter that may have been adsorbed by the biochar during storage. After the removal from the furnace, the preheated biochar was covered with a metal tray and allowed to cool and reduce surface oxidation. The mix and treatment methods for the various samples are shown in Table 2.

Pre-soaking of biochar was done by soaking 50 g of biochar in 200 g of water for a period of 24 h prior to mixing.

Table 2 Mix compositions and CO_2 dosage (internal and/or external carbonation) of 10 types of mortar samples

Sample names	Mix composition					Dry biochar		Pre-soaked biochar		Mortar	
	Cement (kg)	Sand (kg)	Water (kg)	Super-plasticizer (g)	Biochar (g)	Internally dosed	Not dosed with CO_2	Internally dosed	Not dosed with CO_2	Externally dosed	Not dosed with CO_2
Control	1	2.5	400	4.5	0						■
Control-EC										■	
Dry-NC							■				■
Dry-IC						■					■
Dry-EC							■			■	
Dry-I&EC	1	2.45	400	4.5	50	■				■	
PS-NC									■		■
PS-IC								■			■
PS-EC									■	■	
PS-I&EC								■		■	

A shaded box means that the particular condition is present in the biochar sample

Fig. 1 Experimental setup for dosing **a** biochar (dry or pre-soaked, which was kept in the white container), and **b** mortar samples containing various biochar immediately after they were cast in moulds

This quantity of water will count toward the total amount needed for the mortar samples so the containers used for pre-soaking were completely sealed to prevent water loss. In particular, when pre-soaked biochar was exposed to CO_2 dosage in the tank, after 24 h of soaking, its mass before and after the 14-h dosage period was compared; it was found that the total water loss was only 1–5% of the original mass, and this amount of lost water was compensated when the pre-soaked CO_2-dosed biochar was put into the mortar mix. To affect internal carbonation (indicated by "IC" in Table 2), both dry and pre-soaked biochar were subjected to CO_2 dosage. 50 g of each type of biochar was saturated by passing 99.9% CO_2 into a sealed glass tank in which it was kept (Fig. 1a). Investigations by Pu et al. (2021) and Zhang et al. (2021) established the efficacy of using low CO_2 concentrations (that is, ~ 20% (200,000 ppm) or lower) as viable options for curing concrete at ambient pressures, which are practical for future

adoption of ACC as an industrial process. An Aeroqual S500 sensor fit with CO_2 sensor cartridge was used to monitor the CO_2 concentration in the tank; the "saw-tooth" CO_2 dosage method used by Gupta et al. (2018a) was applied in which the internal concentration started with 5000 ppm (or, 0.5%) and was allowed to gradually to 500 ppm (indoor concentration) before more CO_2 was introduced into the tank to bring the concentration back up to 5000 ppm (this is called refilling) (Fig. 1b). This method of dosage is easier to manage without the need for advanced sensor system to keep the internal concentration constant throughout the dosage period. Furthermore, it ensures minimal CO_2 leakage from the tank because fresh doses of CO_2 were introduced only after the additional CO_2 in the tank was absorbed by the mortar samples. In every 24-h period of "saw-toothed" CO_2 dosage, refilling was done for only 7 h, that is, for only 7 h after the first dosage of CO_2 was introduced into the tank (in which the biochar and/or mortar samples were kept), refilling was done whenever the concentration in the tank dropped to 500 ppm; from the 7th hour onwards, the tanks were not refilled and the concentration in the tanks were allowed to fall to 0 ppm (this was achievable because the tanks were air-tight).

Externally carbonated (indicated by "EC" in Table 2) mortar samples were first cast in mold and then immediately put into glass tanks and dosed with CO_2 using the same method mentioned above for internal carbonation of dry or pre-soaked biochar for 24 h in the first day. After this, the tank was opened, the mortar samples were taken out and demolded, and put back in the tank for another 24 h of dosing. After 48 h of dosing, all mortar samples, regardless of whether they contained internally carbonated dry or pre-soaked biochar, were sealed in re-sealable plastic bags during curing for the following 7 days to control evaporative water loss. From the 8th day onwards, all plastic bags were opened to allow further natural carbonation to continue. A summary of the dosing or carbonation procedures for the different types of samples are shown in Fig. 2.

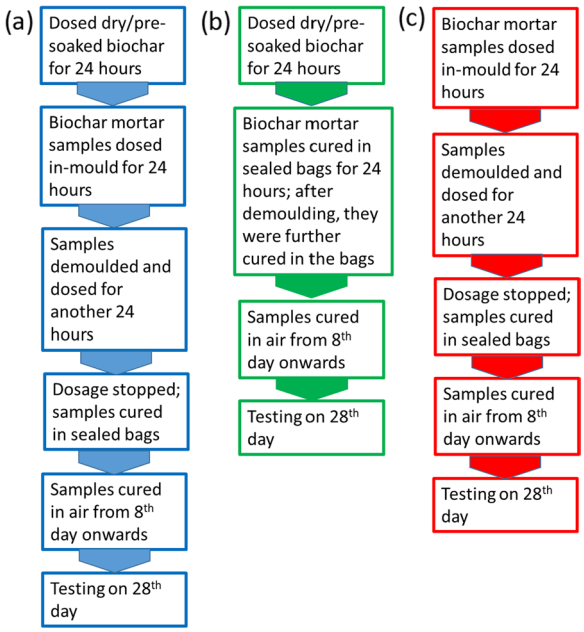

Fig. 2 Duration of CO_2 dosage (accelerated carbonation curing) for: **a** Dry-I&EC and PS-I&EC, **b** Dry-IC and PS-IC, and **c** Dry-EC and PS-EC

3.2 Quantifications of carbonation and hydration products using thermogravimetric analyses (TGA)

We applied the widely used technique of TGA to estimate the masses of the main carbonation and hydration products. All masses were calculated as percentages of a reference mass (M_R), which was either the mortar sample's mass or the mass of the anhydrous cement in the mortar. The mass of $CaCO_3$ was calculated as follows

$$CaCO_3(\%) = \left(M_{630} - M_{830} - \Delta M_{correction(630-830)}\right) \cdot \frac{1}{M_R} \cdot \frac{100.1}{44}.100 \quad (8)$$

TGA measured the loss of mass of the samples between 630 °C (i.e. M_{630}) and 830 °C (i.e. M_{830}) due to the emission of CO_2 from the decomposition of the $CaCO_3$, and the molar mass ratio of $CaCO_3$ to CO_2, $\frac{100.1}{44}$, is the factor used to convert CO_2 mass loss into an estimation of the mass of $CaCO_3$ present before decomposition. The results derived from Eq. (7) must be adjusted for the decrease of total mass due to disintegration of biochar mass in the same temperature ranges. Therefore,

$$\Delta M_{correction(630-830)} = f \cdot (M_{Biochar@630} - M_{Biochar@830}) \quad (9)$$

where $M_{Biochar@630}$ is the mass of the biochar at 630 °C and f is the mass fraction of biochar—dry or pre-soaked—in the mortar sample concerned. The correction term for other temperature ranges could be calculated similarly. From the estimated values of $CaCO_3$, the CO_2 uptake due to the different samples can then be calculated as follows:

Table 3 Four main types of comparisons done on the results of the ten types of mortar samples

			Pre-soaked biochar		Dry biochar		No biochar
			Not dosed	Internally-dosed with CO_2 (IC)	Not dosed	Internally-dosed with CO_2 (IC)	
Mortar	Not dosed	Sample	PS-NC	PS-IC	Dry-NC	Dry-IC	Control
		Comparison type	1	2	1	2	
	Externally-dosed with CO_2 (EC)	Sample	PS-EC	PS-I&EC	Dry-EC	Dry-I&EC	Control-EC
		Comparison type	3	4	3	4	

$$\text{Absolute } CO_2 \text{ absorption}(\%) = (CaCO_3^{Sample} - CaCO_3^{Control}) \cdot \frac{44}{100.1} \quad (10)$$

where $CaCO_3^{Sample}$ and $CaCO_3^{Control}$ is the $CaCO_3$ content in the different samples and control, respectively. CO_2 absorption effectiveness of samples was calculated as follows

$$CO_2 \text{ absorption effectiveness}(\%) = (CaCO_3^{Carbonated\ sample} - CaCO_3^{Non-carbonated\ sample}) \cdot \frac{44}{100.1} \quad (11)$$

Similarly, the CH content can be calculated as

$$CH(\%) = (M_{410} - M_{520} - \Delta M_{correction(410-520))}) \cdot \frac{1}{M_R} \cdot \frac{74.1}{18}.100 \quad (12)$$

where M_{410} and M_{520} are the mass of the mortar sample after being heated to 410 °C and 520 °C, respectively, which signifies the start and the end of the heating phase in which the CH decomposed, and $\frac{74.1}{18}$ is the molar mass ratio of CH to water, which is the factor that converts H_2O mass loss into an estimation of the mass of CH present before decomposition. Finally, the content of total water in the samples, which is a reflection of the amount of CSH, AFm and ettringite, could be estimated as

$$H(\%) = (M_{105} - M_{410} - \Delta M_{correction(105-410)}) \cdot \frac{1}{M_R}.100 \quad (13)$$

where M_{410} and M_{105} are the mass of the mortar sample after being heated to 410 °C and 105 °C, respectively, and it was assumed that by the time the samples were heated to 105 °C, all forms of water in the mix would have been evaporated off from the hydration products.

3.3 Mechanical strength and water sorptivity tests

Compressive strength tests were done in adherence to ASTM C109, on 50 mm–50 mm–50 mm cubes. The standard specified the loading rate to be within the range of 0.9 kNs^{-1} to 1.8 kNs^{-1}. Therefore, the test was run at a compression load of 3000 kN, with a load rate of 1.40 kNs^{-1}. Nine cubes were tested for each of the ten sample types. Flexural strength tests were done according to ASTM C293, whereby samples were cast in the form of rectangular prisms and were subjected to center-point loading. The tests were run at a flexural load of 100 kN, with a load rate of 0.05 kNs^{-1}. Six rectangular prisms were tested for each of the ten sample types.

ASTM C1403 was used to measure the rate of water absorption tests for the mortar samples. To dehydrate the 50 mm–50 mm–50 mm cube samples, they were heated at 110 °C for 24 h. After that, the samples were partially submerged in a tank filled with 3 mm of water, which was covered to minimize water loss through evaporation. To ensure that all surfaces of the samples were uniformly exposed to moisture, the cubes were placed on stainless rods of 3 mm diameter over the entire test period of seven consecutive days. All samples were spaced 12 mm apart from one another, and the samples at the furthermost right and left were placed about 25 mm away from the sides of the tank. Five cube samples were tested for each of the ten sample types. On the first day of the test, the masses of the samples were measured at the 15th minute, first hour, fourth hour and 24th hour. For the subsequent six days, the masses were measured once daily. Prior to each weighing, a damp cloth was used to wipe off the surface water from each sample.

4 Results and analyses

As summarized in Table 3, four types of comparisons were done among the ten types of mortar samples. For example, PS-NC and Dry-NC were evaluated in comparison 1. The following sections were presented with respect to these comparisons. Figure 3 shows the TGA curves of all ten types of mortar, classified into the four types of comparison outlined in Table 3.

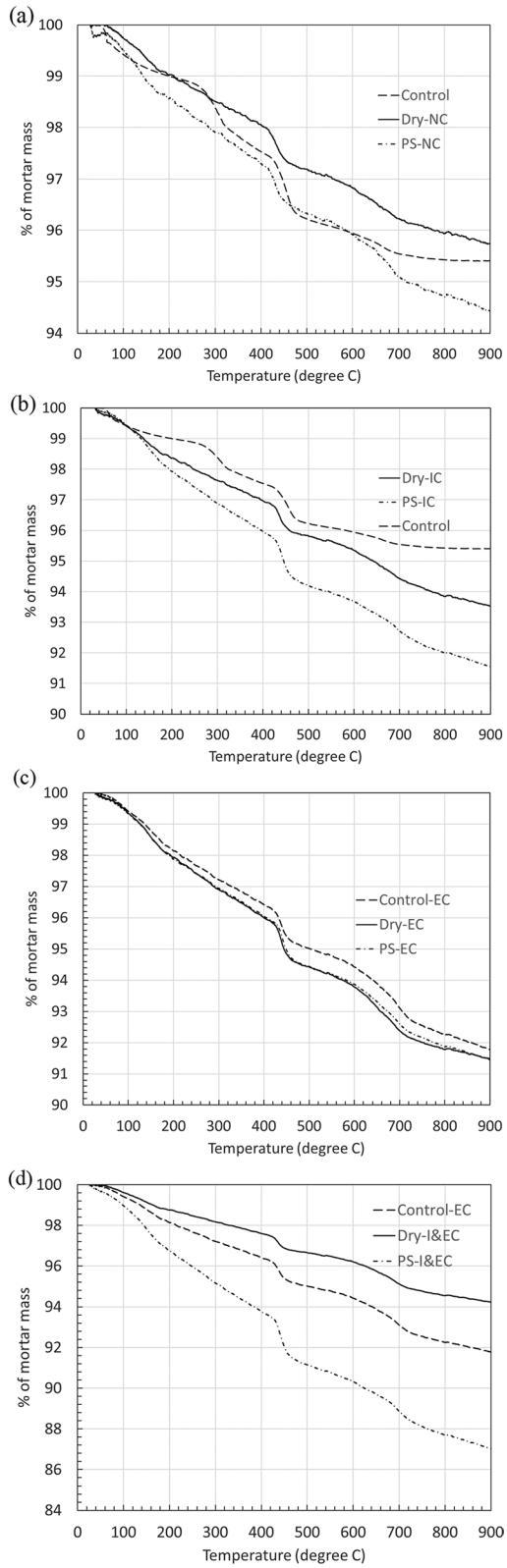

Fig. 3 Thermogravimetric analyses of mortar containing ten different types of biochar in **a** comparison 1, **b** comparison 2, **c** comparison 3, and **d** comparison 4

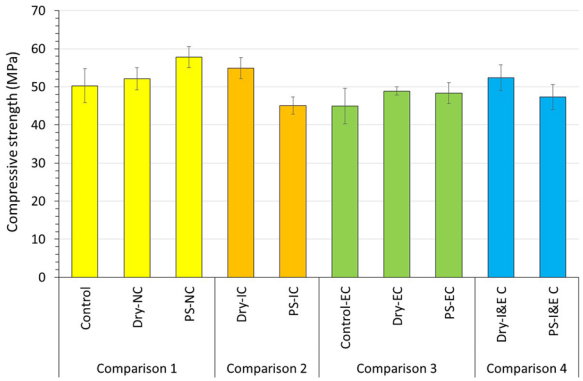

Fig. 4 28-day compressive strengths of 10 different types of mortar samples in this study

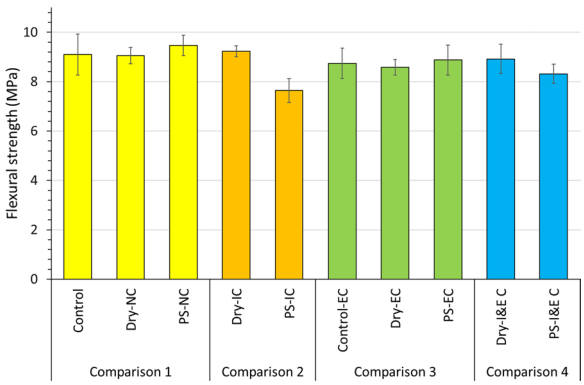

Fig. 5 28-day flexural strengths of 10 different types of mortar samples in this study

4.1 Comparison 1—non-carbonated mortar samples (control, Dry-NC and PS-NC)

In non-carbonated samples, addition of pre-soaked biochar led to significant improvement of 14.9% and 10.9% in 28-day compressive strength ($p = 0.001 < 0.05$, 95% confidence level) over control and Dry-NC, respectively (Fig. 4). This observation is congruent with the earlier findings by Gupta and Kua (2018). But the difference in the flexural strengths of the control, PS-NC and Dry-NC (Fig. 5) was found to be statistically insignificant ($p = 0.210$ and $0.374, > 0.05$). Addition of biochar can only increase flexural and tensile strengths if the surface roughness afforded by the biochar particles anchors them into the surrounding matrix, hence acting as connection points in the matrix; this not only reduces the relative displacement between regions in the matrix, but also reduces the formation and propagation of cracks through these layers (Kua et al. 2020).

Figure 6 compares the overall water sorptivity, and Table 4 compares the initial and secondary sorptivity values, of the three samples; while no statistically

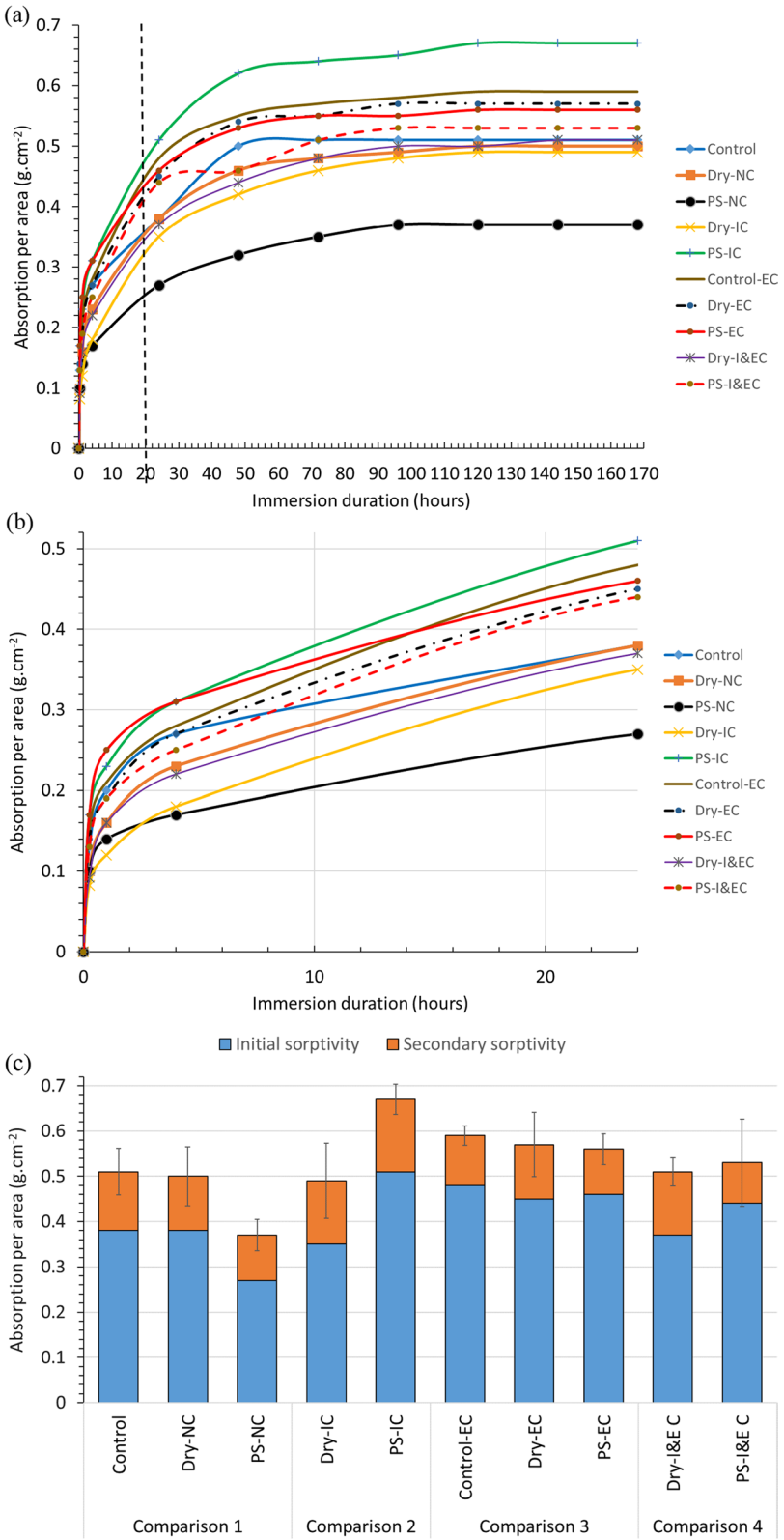

Fig. 6 Comparisons of the **a** Overall water sorptivity over time, **b** initial water sorptivity over time (first 24 h), and **c** average total initial and secondary water sorptivity of the 10 mortar samples after 7 days (or 168 h). The dotted line in **a** indicates the initial sorptivity mark, and the sorptivity of the region to the left of this dotted line is shown in **b**

Table 4 Initial and secondary sorptivity comparisons for all mortar samples

Sample types	Mean Initial Sorptivity in first 24 h (g cm^{-2})	Mean Secondary Sorptivity (g cm^{-2})
Control	0.38	0.13
Dry-NC	0.38	0.12
PS-NC	0.27	0.10
Dry-IC	0.35	0.14
PS-IC	0.51	0.16
Control-EC	0.48	0.11
Dry-EC	0.45	0.12
PS-EC	0.46	0.10
Dry-I&EC	0.37	0.14
PS-I&EC	0.44	0.09

significant difference was found between control and Dry-NC, PS-NC shows distinctly lower (about 26%) initial and secondary sorptivity than control. This result is again consistent with those from Gupta and Kua (2018). Mortar permeability was mainly determined by the porosity of cementitious matrix instead of the aggregates' (Espinoza-Hijazin and Lopez 2011). Biochar pores absorbed part of the free water in the binder gel, resulting in lower water loss from the matrix around the biochar particles due to evaporation and bleeding, which in turn yielded a more compact pore structure with lower connectivity in the pore network. This subsequently reduces the "conduits" for infusion of water into the hardened mortar. Furthermore, the waterlogged biochar particles act "reservoirs" that released portion of the absorbed moisture to the matrix whenever there was a water concentration gradient between biochar and the surrounding matrix (Gupta and Kua 2018). This sustained hydration and resulted in a denser microstructure and this can be seen in Fig. 7a. Lastly, the biochar particles acted as filler that reduced the overall permeability of the mortar matrix (Mrad and Chehab 2019). In summary, the two main mechanisms by which the pre-soaked and dry biochar enhanced hydration were the filler effect and moisture regulation (which balanced between absorption of free water and realizing the "reservoir" effect).

The key difference between dry and pre-soaked biochar in these two mechanisms was that pre-soaking enables saturation of the biochar pores before mixing, and because the total amount of water in the mortar

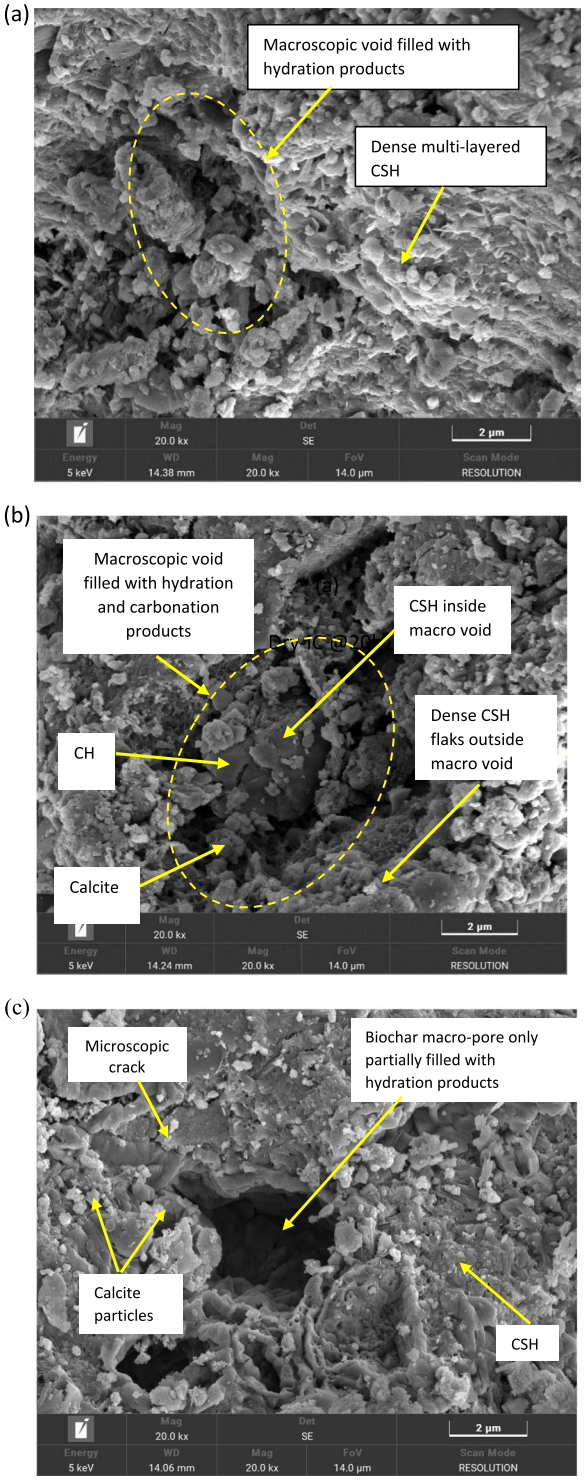

Fig. 7 Microstructure of matrix regions around macroscopic air void or biochar pore in **a** PS-NC, **b** Dry-IC, and **c** PS-IC

Table 5 Contents of products of hydration and carbonation, as calculated from thermogravimetric analytical data

Types of comparison	Sample types	$CaCO_3$ (%), relative to mass of mortar samples	$CaCO_3$ (%), relative to mass of anhydrous cement	H (%), relative to mass of mortar samples	CH (%), relative to mass of mortar samples	Absolute CO_2 adsorption (%)	Carbonation effectiveness (%)
1	Control	0.90	1.40	1.90	5.38	0.00	0.00
	Dry-NC	1.58	2.45	1.72	3.61	0.46	0.00
	PS-NC	2.24	3.47	2.21	4.06	0.91	0.00
2	Dry-IC	2.85	4.42	2.44	4.86	1.33	0.87
	PS-IC	3.30	5.12	3.50	7.37	1.64	0.72
3	Control-EC	4.37	6.77	3.02	5.87	2.36	2.36
	Dry-EC	3.73	5.78	3.36	6.56	1.93	1.46
	PS-EC	3.83	5.94	3.31	6.72	2.00	1.08
4	Dry-I&EC	3.20	4.96	2.02	3.92	1.57	1.10
	PS-I&EC	5.21	8.08	5.22	10.86	2.94	2.02

Absolute CO_2 adsorption was calculated with respect to the control (relative to mass of anhydrous cement), whereas carbonation effectiveness was calculated with respect to corresponding non-carbonated samples (relative to mass of anhydrous cement)

mix was kept unchanged, the free water in the matrix outside the biochar pores was lower than if the biochar was dry; this reduced the formation of air voids due to evaporative water loss and caused the pre-soaked biochar to have a better internal curing effect than dry biochar, thus leading to more compact microstructure (Gupta and Kua 2018). As a result, the compressive strength of PS-NC is higher, and its water sorptivity is lower than control. Two types of sorptivity were examined—initial sorptivity, which occurred in the first 24 h (or, second = 147) of test due to the suction of fine capillary pores, and secondary sorptivity, which occurred from day 1 onwards due to absorption of water into macroscopic pores and air voids. Table 4 shows that enhanced hydration caused by pre-soaked biochar effectively reduced the total amount of fine capillary pores and subsequent macroscopic air voids.

Although Dry-NC was stronger in compression, its water sorptivity was statistically the same as control's—this can be attributed to the higher pore tortuosity of Dry-NC. Ahmad et al. (2005) examined the relationships among porosity, permeability, tortuosity and water-cement (w/c) ratio; they found that between w/c ratios of 0.4 and 0.5, the variations in permeability of samples with different fine and coarse aggregate proportions were about 40% but the variations in tortuosity were 62.9%. Higher pore tortuosity is associated with higher compressive strength of mortar because it leads to higher surface energy needed for cracks to propagate through the bulk material.

The ability of pre-soaked biochar to enhance hydration manifested in the higher combined water, H (%), content that includes CSH, AFm and ettringite. Although Dry-NC had higher compressive strength than control, the former's H% was found to be close to the latter's. However, one couldn't differentiate between the CSH content of Dry-NC and control from H% data (Fig. 3a); more studies are therefore needed. PS-NC and Dry-NC were found to have about 2.49 times and 75.6% more CO_2 than control, and this can be attributed to the additional CO_2 adsorbed on the surfaces of the biochar from air (for Dry-NC) and both air and water (for PS-NC). As shown in Table 5 and Fig. 8, in the absence of ACC, putting pre-soaked biochar in cementitious mix can result in reasonably high natural carbonation rate. This point was further elaborated in Sect. 4.5.

4.2 Comparison 2—mortar containing internally carbonated biochar (control, Dry-IC and PS-IC)

The reaction products in the mortar depend on the confluence of carbonation and hydration at any point in time, depending on the specific reactivity of the phases present and CO_2 availability (Cizer et al. 2009), and some of the key by-products are different CSH phases characterized by different Ca/Si ratios that could co-exist (Zajac et al. 2022a). In particular, post-carbonation hydration reactions have a pronounced effect on the phase composition—for example, carbonated systems rich in the CSH phase with low Ca/Si ratio (CSH_{low}) and silica gel can be transformed into systems dominated by the CSH with high Ca/Si ratio (CSH_{high}) during normal cement hydration (Zhan et al. 2019; Liu et al. 2021; Zajac et al. 2022a). Increasing Ca/Si ratio has varying effect on the mechanical properties of CSH pastes (Im et al. 2023). As Ca/Si increases, the density of the CaO layers increases and silicate chains shortens—the former increases the nano- and micro-mechanical properties (Li et al. 2020; Geng et al.

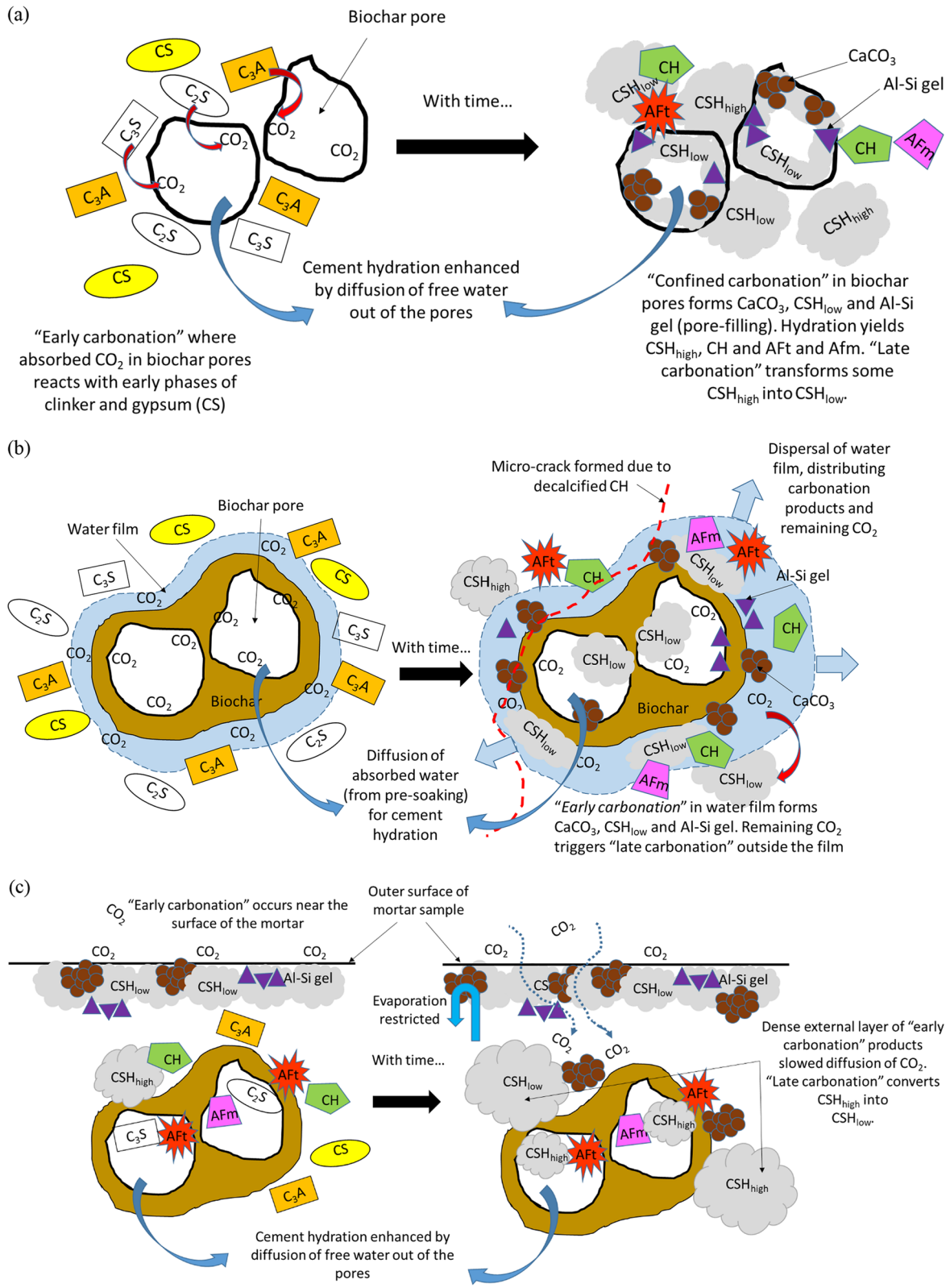

Fig. 8 Schematics of proposed models that explained the combined effects of "early carbonation", "late carbonation", hydration and various physical processes in **a** Dry-IC, **b** PS-IC, **c** Dry-EC, **d** PS-EC, and **e** PS-I&EC

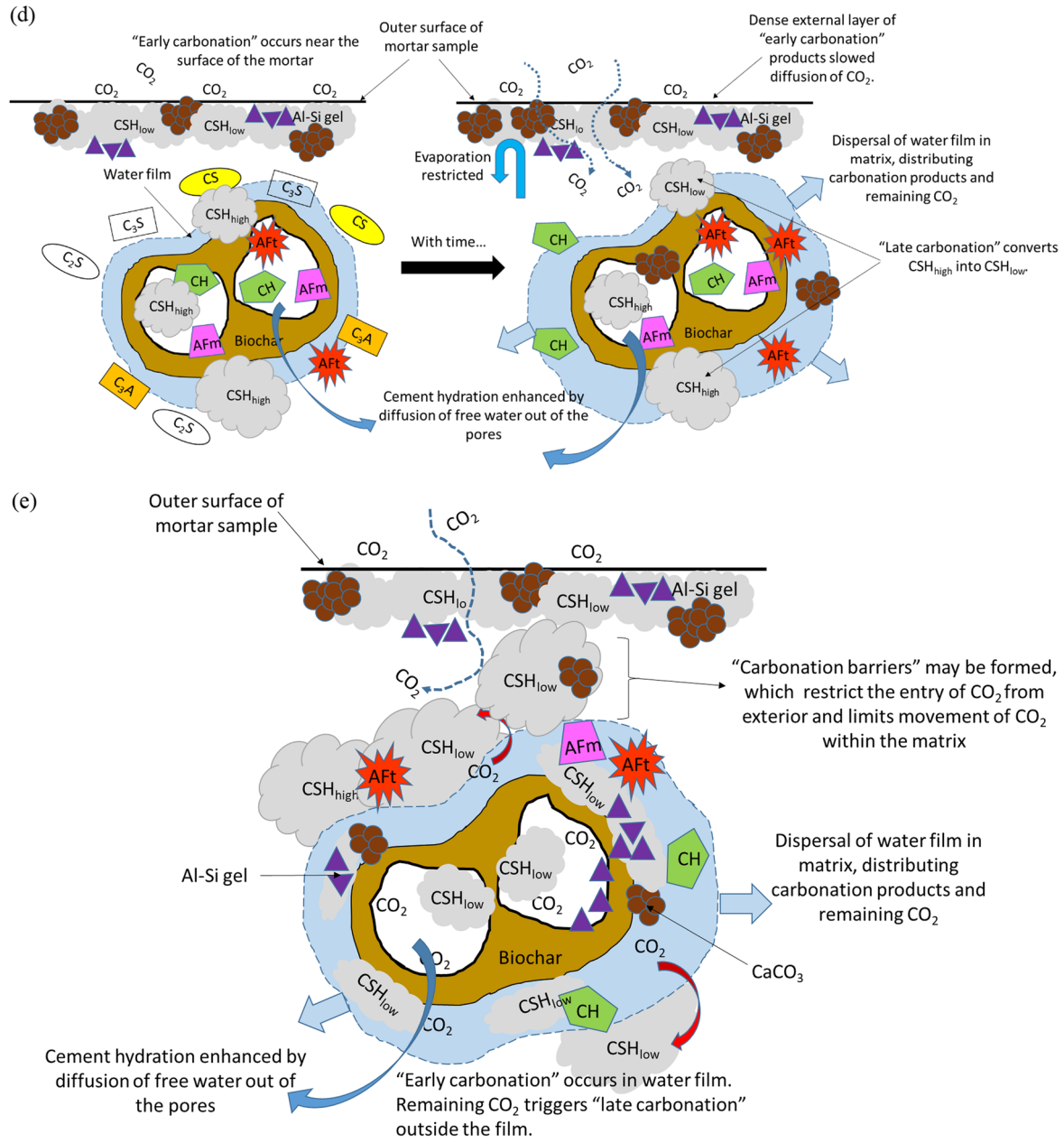

Fig. 8 continued

2017), whereas the latter decreases the macro-mechanical properties (Abdolhosseini Qomi et al. 2014; Manzano et al. 2009). Furthermore, higher H_2O/Si ratio caused by higher moisture content in the CSH pastes in the presence of higher Ca/Si ratios can also hinder the ability of the solid phase to resist external loading at the macroscopic scale (Zajac et al. 2022b).

As shown in Fig. 8a, by confining the CO_2 within and around the biochar pores (that is, "confined carbonation"), the products of carbonation—namely, CSH_{low}, alumina-silica gel and $CaCO_3$—were confined in the pores, resulting in pore-filling (Fig. 7b). In the meantime, enhanced hydration occurred in the matrix around the biochar through the aforementioned mechanisms of moisture regulation by the pores. As shown qualitatively in Fig. 8a, "late carbonation" initiated by any remaining CO_2 that flowed out of the pores with the moisture reacted with available CH to yield $CaCO_3$ and CSH_{low} (partially converted from CSH_{high}). This localized accumulation of carbonation products

explained the higher compressive strength of Dry-IC, compared to control ($p = 0.001 < 0.05$) (Fig. 4), and higher H% in Dry-IC compared to control (2.44% compared to 1.90%) (Table 5).

Despite the high H content, Dry-IC's lower CH content—4.86% compared to 5.38% (for control)—indicated that certain degree of decalcification had occurred as a result of the aforementioned late carbonation (Fig. 3b). Finally, the lack of significant difference between the flexural strength of Dry-IC and control ($p = 0.91 > 0.05$) is consistent with the observations in the last section.

On the contrary, PS-IC was found to have 16.04% significantly lower flexural strength ($p = 0.02 < 0.05$) and 10.33% lower compressive strength ($p = 0.01 < 0.05$) than control; this corresponds to being 21.7% lower in compressive strength ($p = 0.00 < 0.05$) and 17.23% lower in flexural strength than Dry-IC ($p = 0.02 < 0.05$). This difference in the mechanical properties of Dry-IC and PS-IC could be explained using the two variants of internal carbonation in Figs. 8a and 6b. Pre-soaked biochar in PS-IC was exposed to CO_2 when it was water-logged before it was deployed in the mortar mix, which resulted in CO_2 being predominantly dissolved and concentrated in the water film (Fig. 8b). This initiated "early carbonation" in this water layer within the binder gel. As the water film dispersed in the mortar matrix, promoted by the "reservoir effect" (that is, internal curing), any remaining CO_2 concentrated in the water could go on to decalcify any CH and/or CSH that was formed from hydration enhanced by the water regulation effects and filler effect of the pre-soaked biochar. The concentration of decalcified CH and/or CSH in regions with this CO_2-concentrated water, including the interfacial transition zone (ITZ), created weak zones that facilitated the formation and growth of microscopic cracks through the matrix (as shown in both Figs. 7c and 8b).

However, as shown in Fig. 6 and Table 4, there was no significant difference in overall water sorptivity between Dry-IC and control (p-value $= 0.579 > 0.05$), which implied that while pore-filling (due to "confined carbonation") and enhanced hydration in Dry-IC contributed significantly to its compressive strength, the $CaCO_3$ formed in the biochar pores and the matrix were unable to sufficiently block the ingress of water through the capillary and macro-pores when the sample was submerged over extended period of time. One possible reason was that excess amount of dissolved unreacted CO_2 on the biochar surface caused some of the $CaCO_3$ to be turned into soluble $Ca(HCO_3)_2$. Another possible reason was pore-filling resulted in higher tortuosity of the pore network in Dry-IC compared to that in the control, which increased the surface energy required for cracks to propagate through the matrix, but this phenomenon would not affect the infiltration of water through the fine capillary pores within the densely formed hydration and carbonation products over time.

Results on water sorptivity of PS-IC were consistent with the compressive and flexural strength results—it was 31.37% more permeable to water than the control and Dry-IC (Fig. 6); this was mainly due to higher capillary porosity (initial sorptivity) of the PS-IC (34.21% higher than control and 36.73% higher than Dry-IC), even though its secondary sorptivity was similar to those of control and Dry-IC (Table 4).

Finally, the higher $CaCO_3$ content of PS-IC (15.79% higher than that in Dry-IC) indicated higher CO_2 absorbed by the pre-soaked biochar. This could be understood from the difference in the production and preparation process that pre-soaked biochar went through, compared to dry biochar—after biochar was produced, it absorbed CO_2 from the surrounding air; pre-soaked biochar was kept in water for additional 24 h and this would have enabled the water film in the proximity of the biochar pores to capture more CO_2 compared to the amount that could be adsorbed in the pores in Dry-IC.

Furthermore, the higher CH content (7.37%, compared to 5.38% in control) and H content (3.50%, compared to 1.90% in control) indicated that any decalcification of CH and/or CSH had been more than compensated by the enhanced hydration due to the internal curing effect afforded by the waterlogged pores.

4.3 Comparison 3—externally carbonated mortar (control-EC, Dry-EC and PS-EC)

No significant difference was found between the compressive strengths of PS-EC and Dry-EC ($p = 0.769 > 0.05$). Both were also similar in compressive strength to control-EC ($p = 0.30$ for Dry-EC, and $p = 0.25$ for PS-EC). However, compared to control, the compressive strength of control-EC was found to be significantly lower (p-value $= 0.012 < 0.05$). These results differed from the results obtained by Rostami et al. (2012), who found that ACC using external carbonation approach improved the 28-day compressive strength of cement mortar. The difference between their study and this study was that Rostami et al. carried out carbonation curing for only 2 h (after 18 h of air curing). As mentioned above, prolonged exposure to CO_2 could disintegrate the CH and CSH within the matrix (as indicated in Figs. 8c and 6d), and excessive carbonation would also convert part of the $CaCO_3$ into water soluble $Ca(HCO_3)_2$, thus giving rise to a more porous matrix with lower mechanical strength.

Similar to the trend in compressive strength, no significant difference was found between the flexural strengths of PS-EC and Dry-EC ($p = 0.311 > 0.05$) (Fig. 5). There was also no significant difference between PS-EC and

control-EC ($p = 0.38 > 0.05$), and between Dry-EC and control-EC ($p = 0.23 > 0.05$). These results showed that when the biochar was not dosed, the properties of the mortar were determined primarily by external carbonation; however, the lack of difference in the hydration enhancement effect of the dry and pre-soaked biochar was counter-intuitive. As described above, setting the water-cement ratio constant across all sample types meant that using pre-soaked biochar indirectly reduced the amount of free water added into the matrix around the biochar, which reduced the rate of evaporative water loss; this phenomenon would be less effective when dry biochar was used. However, as shown in Figs. 8c and 6d, the layer of "early carbonation" products near the surface of the externally CO_2-dosed samples could have limited evaporative water loss, thus reducing the difference between the effects of dry biochar and pre-soaked biochar.

Figure 6 shows consistency with the trend in mechanical strengths—control-EC was significantly more permeable than control, and both Dry-EC and PS-EC were marginally less permeable than control-EC. The permeability of all three samples was determined mainly by the layer of "early carbonation" products; however, the aforementioned enhanced hydration due to the presence of biochar particles developed a denser matrix that would have restricted the ingress of water and CO_2 into the matrix for carbonation, thus resulting in control-EC having 14.64% and 12.36% higher $CaCO_3$ content than Dry-EC and PS-EC respectively (Table 5 and Fig. 3c). Correspondingly, control-EC was able to absorb more CO_2 than the other two samples. Enhanced hydration in the presence biochar also resulted in control-EC to have significantly lower H and CH contents than Dry-IC (by 11.26% for H and by 11.69% for CH) and PS-EC (by 9.60% for H and by 14.41% for CH).

4.4 Comparison 4—externally carbonated mortar containing internally carbonated biochar (control-EC, Dry-I&EC and PS-I&EC)

4.4.1 Dry-I&EC, Dry-IC and Dry-EC

In general, the properties of Dry-I&EC are intermediate to those of Dry-EC and Dry-IC, and those of PS-I&EC are intermediate to those of PS-EC and PS-IC. Specifically, as shown in Fig. 4, Dry-I&EC was 7.16% higher in compressive strength than Dry-EC and this difference was found to be marginally significant ($p = 0.05$); however, it was statistically similar to Dry-IC ($p = 0.09 > 0.05$). In contrast with Dry-IC (Fig. 8a), "early carbonation" in Dry-EC (Fig. 8c) occurred near the external surface area of the mortar cubes, and so pore-filling by "early carbonation" products was absent in Dry-EC; instead, "late carbonation" in which the remaining CO_2 molecules that diffused deeper into the matrix decalcified CH and/or CSH, developed a more porous matrix in Dry-EC. This explained Dry-EC's 10.93% significantly lower compressive strength ($p = 0.00 < 0.05$), and 7.04% significantly lower in flexural than Dry-IC ($p = 0.04 < 0.05$). Correspondingly, Dry-EC had 14.04% higher water sorptivity than Dry-IC.

With respect to flexural strength, all three types of samples were found to be statistically the same (Fig. 5). Water sorptivity of Dry-IC, Dry-I&EC and Dry-EC was found to be 0.49, 0.51 and 0.57 gcm^{-2}, respectively (Fig. 6) and no significant difference was found among these values. The initial sorptivity of Dry-I&EC and Dry-IC was similar, whereas Dry-I&EC was 21.62% lower than Dry-EC in initial sorptivity but 16.67% higher in secondary sorptivity.

Absorbing CO_2 over a larger external surface area enabled Dry-EC to develop more $CaCO_3$ (by 30.88%) than Dry-IC. It is counterintuitive that even with additional CO_2 dosage (that is, internal carbonation followed by external carbonation), Dry-I&EC did not have higher $CaCO_3$ content than Dry-EC; in fact, it was about 16.56% lower. A likely reason was that excessive CO_2 that diffused through the layer of near surface "early carbonation" products (Fig. 8c) dissolved in the free water available within the biochar pores that already contained dissolved CO_2 or $CaCO_3$ from "early carbonation" in and around the biochar pores, thus causing the biochar pores to become locations with higher acidity that could set off this reaction

$$CO_2(aq) + H_2O \rightleftharpoons H_2CO_3 \rightleftharpoons HCO_3^- + H^+ \rightleftharpoons CO_3^{2-} + 2\,H^+ \quad (14)$$

Increased CO_2 availability produced high amount of carbonic acid (H_2CO_3) and more free H + ions would be released into the mortar mix and this creates an imbalance in the above equation. Maintaining chemical equilibrium necessitates carbonate ions in the mortar mix reacting with the H^+ ions to yield soluble bicarbonate ions. This reaction was expected to have decreased the $CaCO_3$ content of Dry-I&EC. More studies are needed to confirm this deduction in the future.

Finally, the lower CH content of Dry-I&EC—27.21% lower than control and 33.29% compared to control-EC—was an indication that a substantial amount of the CO_2 absorbed in the biochar pores was involved in the "late carbonation" (Fig. 3d). Together with the additional CO_2 from exterior that diffused into the matrix through the layer of near surface "early carbonation" products, the total degree of CH decalcification in Dry-I&E was expected to be higher than Dry-EC. Furthermore, "confined carbonation" in the biochar pores of Dry-IC used up relatively more water in the pores, thus

rendering them less effective in their water regulation function; this could explain the fact that Dry-IC has 37.70% lower H than Dry-EC. This phenomenon does not contradict the observation that Dry-IC is higher in mechanical strength because, as shown in Fig. 7c, the highly dense matrix of Dry-EC could still yield lower strength values due to the formation and development of micro-cracks as a result of localized CH or CSH decalcification from "late carbonation".

In general, the results provided evidence that the combined actions of internal carbonation and hydration have a more dominant effect on the permeability of the matrix.

4.4.2 PS-I&EC, PS-IC and PS-EC

No significant difference was found between the compressive strength of PS-I&EC and PS-IC ($p = 0.12 > 0.05$), and between PS-I&EC and PS-EC ($p = 0.65 > 0.05$). Similarly, no significant difference was found among the flexural strengths of all three samples. However, water sorptivity of PS-I&EC was found to be significantly lower than that of PS-IC ($p = 0.01 < 0.05$), even though there was no significant difference found between that of PS-EC and PS-I&EC ($p = 0.55 > 0.05$). Table 5 shows that the $CaCO_3$ content of PS-I&EC was the highest among the three samples, which was opposite to the situation with Dry-I&EC. The reason was that, as illustrated in Fig. 8d, "early carbonation" occurred mainly in the water film and dispersed water around the biochar particles. As a result of such dispersion, the localized acidity level would be lower than in the biochar pores of Dry-I&EC, thus reducing the conversion of the CO_3^{2-} ions into HCO_3^- ions. Moreover, this dispersion of CO_2-concentrated water from the pre-soaked biochar into the surrounding matrix, as part of the internal curing process, was expected to increase the rate of carbonation, thus increasing the $CaCO_3$ content of the areas it reached. However, this deduction necessitates further investigation in future studies.

Overall, as shown in Figs. 4, 5 and 6, PS-IC has the lowest compressive and flexural strength, and the highest water sorptivity. Specifically, the compressive strength of PS-IC was 7.10% lower ($p = 0.02 < 0.05$) and flexural strength 16.23% lower than that of PS-EC ($p = 0.03 < 0.05$), despite having 5.74% higher H and 9.68% higher CH than PS-EC; water sorptivity of PS-IC was 19.64% higher than that of PS-EC, which corresponded to the trend in the mechanical strength. This difference could be attributed to the formation of "early carbonation" products and decalcification in various concentrated spots, including around the ITZ. In contrast, external carbonation of PS-EC resulted in carbonation that was more widely distributed throughout the matrix (Fig. 8d), which avoided or reduced the formation of concentrated weak spots. More uniform carbonation (early and late) across larger volume of materials also caused PS-EC to have higher $CaCO_3$ content than PS-IC. The layer of near surface "early carbonation" products in PS-EC limits CO_2 diffusion so the said increased carbonation was due mostly to "late carbonation" where CH and/or CSH were decalcified to yield $CaCO_3$, hence leading to lower CH in PS-EC. On the other hand, "early carbonation" in PS-IC was higher (Fig. 8b) and coupled with enhanced hydration by the pre-soaked biochar, its CH content was higher than that found in PS-EC.

In contrast with Dry-I&EC, PS-I&EC has the highest CH content of all sample types in this study. Other than having a high degree of internal curing by the pre-soaked biochar in the PS-I&EC that led to enhanced hydration, there could be another reason. With reference to Fig. 8e, when CO_2-rich water around the pre-soaked CO_2-dosed biochar dispersed and initiated "early carbonation" in the proximity and if these locations coincided with "early carbonation" sites near the mortar surface, "carbonation barriers" would be formed that restricted the entry of CO_2 from exterior, and/or limited the spreading of this CO_2 within the matrix. This would have the effect of limiting "late carbonation", thus resulting in less CH and CSH decalcification compared to PS-IC and PS-EC.

4.5 Typology of ACC—comparison of absolute carbon dioxide absorption and carbonation effectiveness per CO_2 dosage duration

As shown in Fig. 9a and b, two types of typologies were proposed for biochar mortar, using two types of CO_2 absorption measurement (equations). It is worth mentioning that because carbonation effectiveness measures the additional CO_2 absorption due to carbonation for every sample type by comparing between the carbonated and the non-carbonated samples (for example, comparing Dry-IC with Dry-NC, and comparing PS-EC with PS-NC). A lower carbonation effectiveness does not mean worse carbon sequestration capability, because this might be caused by a relatively high CO_2 absorption capability of the non-carbonated samples, which may be caused by the presence of biochar (dry or pre-soaked). Both these CO_2 absorption measurement qualities were normalized to the carbonation duration (in hours) to which the respective samples were subjected; in other words, we also measured carbonation efficiency, which is defined as carbonation effectiveness per carbonation duration.

The four quadrants in Fig. 9 were defined in relative terms—the levels of strength (high or low) were defined with respect to the strength of the control, and the levels

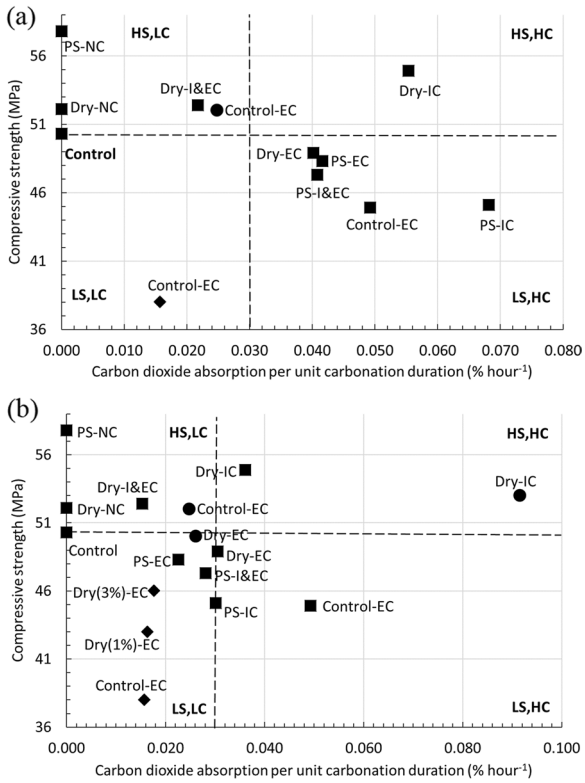

Fig. 9 Typology of Accelerated Carbonation Curing, using different types of biochar as tuning agent. **a** represents the absolute CO_2 absorption per unit dosage duration of each CO_2-dosed sample relative to control, whereas (**b**) represents the increase in CO_2 absorption (%) of each sample relative to the non-carbonated version of itself (that is, carbonation effectiveness) per unit carbonation duration. Data from this study (■), Gupta (2021; ●) and Gupta et al. (2021; ♦) were compared. Four general typologies were identified: "low strength, low carbonation" (LS, LC), "high strength, low carbonation" (HS, LC), "low strength, high carbonation" (LS, HC), and "high strength, high carbonation" (HS, HC)

of carbonation (high or low) can be defined according to any set target. In Fig. 9, 0.03%/hour was used as an arbitrary target and any values higher than it was considered higher carbonation and vice versa. In Fig. 9a, it is evident that Dry-IC could increase both compressive strength and carbonation efficiency with respect to the control and the carbonation target (0.03%/hour); this implies that internally carbonated dry biochar was the most efficient way to augment ACC in cementitious mortar. This conclusion was also supported by the results obtained by Gupta (2021) in Fig. 9b. Samples containing carbonated pre-soaked biochar (PS-EC, PS-IC and PS-I&EC) were able to increase carbonation but at the expense of compressive strength (they are in the "low strength, high carbonation" quadrant). However , PS-EC was grouped under the "low strength, low carbonation" quadrant in Fig. 9b, due to relatively high CO_2 absorption in PS-NC (0.91% of the anhydrous cement mass, as shown in Table 5).

These results imply that if the aim is to increase carbonation to the maximum possible, and high compressive strength is not necessary (for example used in non-load bearing wall of less than 40 MPa in buildings), then using internally carbonated pre-soaked biochar is the preferred approach. The significance of these conclusions for Dry-IC and PS-IC is that carbonating dry and pre-soaked biochar is technically easier to implement on commercial scale than carbonating cast concrete components that are larger; therefore, this implies that Dry-IC and/or PS-IC might be considered as an alternative to the conventional method of ACC (using the equivalent of control-EC).

A combination of external and internal carbonation (Dry-EC and Dry-I&EC) could increase compressive strength but they drastically decreased carbonation. In particular, Dry (1%)-EC and Dry (3%)-EC from Gupta et al. (2021) were found to reside in the "low strength, low carbonation" quadrant because of the long carbonation period (28 days). The small difference between the carbonation effectiveness of Dry (1%)-EC and Dry (3%)-EC (in Fig. 9b) showed that when carbonation is external, increasing the quantity of biochar in the mortar mix will not produce substantial increase in carbonation.

Finally, the widely differing positions of control-EC in Fig. 9 underlined the fact that carbonation efficiency of this more conventional way of ACC can differ substantially according to a host of factors—for example, total carbonation duration, CO_2 concentration during carbonation, and the presence of pre-carbonation treatment. Specifically, the control-EC in this study was exposed to carbonation right after casting when the samples were in the mold, and this early exposure (thus absence of pre-carbonation treatment) was expected to have increased the total amount of CO_2 sequestered.

5 Conclusions

This study set off to quantify and compare the compressive strength, flexural strength, water sorptivity and absolute CO_2 adsorption efficiency of cementitious mortar containing dry and pre-soaked biochar subjected to internal and/or external carbonation. By examining patterns in these qualities and collating recent results from the literature, we understood how these different types of biochar can augment ACC. It was found that Dry-IC increased both the compressive strength and carbonation efficiency of ACC. This increase in strength could primarily be explained by five interrelated qualitative models of combined carbonation-hydration in biochar mortar (Fig. 8); specifically, "early carbonation" and "confined carbonation" within the pores of the dry biochar caused pore-filling and subsequent reduction in mortar permeability. However, if further increase in carbonation is

required with certain tolerance for reduction in compressive strength, then PS-IC could be used instead. These two methods are easier to implement than the conventional ACC (that is, control-EC).

The quantity of biochar, size of mortar samples and size of dosing tanks used in this study were of bench top scale; furthermore, 99.9% industrial grade CO_2 was used for the dosage. If the proposed methods of ACC were to be employed over larger commercial scales, future studies should involve dosing actual precast concrete members (which contain different types of biochar samples) with exhaust gas from an onsite source (such as a generator) in a dosage chamber of actual size. By varying the dosage duration of each batch of these precast concrete members and conducting this experiment over an extended period of time, one can gain useful insight into the optimal duration that can yield the highest carbonation efficiency while keeping compressive strength to a certain minimum value. Nonetheless, on the whole, the ACC typology proposed in this study could hopefully accelerate more studies and eventually industrial adoption of ACC methodologies that apply biochar as a tuning agent.

Abbreviations

ACC	Accelerated carbonation curing
Control-EC	Control mortar subjected to external carbonation
Dry-NC	Mortar containing dry biochar and mortar not subjected to any carbonation
PS-NC	Mortar containing pre-soaked biochar and mortar not subjected to any carbonation
Dry-EC	Mortar containing dry biochar and mortar subjected to external carbonation
PS-EC	Mortar containing pre-soaked biochar and mortar subjected to external carbonation
Dry-IC	Mortar containing dry biochar subjected to internal carbonation
PS-IC	Mortar containing pre-soaked biochar subjected to internal carbonation
Dry-I&EC	Mortar containing dry biochar subjected to internal carbonation, and mortar subjected to external carbonation
PS-I&EC	Mortar containing pre-soaked biochar subjected to internal carbonation, and mortar subjected to external carbonation

Variables

$\Delta M_{correction(x-y)}$	Decrease of total mass due to disintegration of biochar mass in the temperature ranges between x and y
M_x	Mass of mortar samples at temperature x
f	Mass fraction of biochar in mortar sample

Acknowledgements
The authors would like to acknowledge with deep gratitude the Department of the Built Environment and College of Design and Engineering for providing the funding (E-471-00-0009-02) to support this work.

Author contributions
HWK: Conceptualization; Experimentation; Data curation; Formal analysis; Methodology; Validation; Visualization; Roles/Writing—original draft; Writing—review & Editing; Project administration; Resources. ST: Experimentation; Data curation; Formal analysis; Methodology; Validation; Visualization; Roles/Writing—original draft. Both authors read and approved the final manuscript.

Funding
This study was supported by Department of the Built Environment and College of Design and Engineering (E-471-00-0009-02).

Availability of data and materials
Data will be shared upon request.

Declarations

Ethics approval and consent to participate
Not applicable.

Consent for publication
Not applicable.

Competing interests
All authors do not have any competing interests.

Author details
[1]Department of the Built Environment, College of Design and Engineering, National University of Singapore, Singapore, Singapore.

Received: 31 December 2022 Revised: 24 May 2023 Accepted: 28 May 2023
Published online: 29 June 2023

References

Abdolhosseini Qomi MJ, Krakowiak KJ, Bauchy M, Stewart KL, Shahsavari R, Jagannathan D, Brommer DB, Baronnet A, Buehler MJ, Yip S, Ulm FJ (2014) Combinatorial molecular optimization of cement hydrates. Nat Commun 5(1):1–10

Ahmad S, Azad AK, Loughlin KF (2005) A study of permeability and tortuosity of concrete. In 30th conference on our world in concrete and structures, Vol. 45, 23–30

Ahmad S, Tulliani JM, Ferro GA et al (2015) Crack path and fracture surface modifications in cement composites. Fracture Struct Integrity 9(34):524–533

Ali M, Abdullah MS, Saad SA (2015) Effect of calcium carbonate replacement on workability and mechanical strength of portland cement concrete. Adv Mater Res 1115:137–141

Ashraf W, Olek J (2016) Carbonation behavior of hydraulic and non-hydraulic calcium silicates: potential of utilizing low-lime calcium silicates in cement-based materials. J Mater Sci 51:6173–6191

Cao ML, Ming X, He KY et al (2019) Effect of macro-, micro- and nano-calcium carbonate on properties of cementitious composites—a review. Materials (basel, Switzerland) 12(5):781

Choi WC, Yun HD, Lee JY (2012) Mechanical properties of mortar containing biochar from pyrolysis. J Korea Inst Struct Maint Inspection 16(3):67–74

Cizer Ö, Van Balen K, Van Gemert D, Elsen J (2009) Competition between carbonation and hydration on the hardening of calcium hydroxide and calcium silicate binders. WTA Publications, Karlsruhe, pp 353–368

Creamer AE, Gao B, Zhang M (2014) Carbon dioxide capture using biochar produced from sugarcane bagasse and hickory wood. Chem Eng J 249:174–179

Dissanayake PD, You S, Igalavithana AD, Xia Y, Bhatnagar A, Gupta S, Kua HW, Kim S, Kwon JH, Tsang DC, Ok YS (2020) Biochar-based adsorbents for carbon dioxide capture: a critical review. Renew Sustain Energy Rev 119:109582

Espinoza-Hijazin G, Lopez M (2011) Extending internal curing to concrete mixtures with W/C higher than 0.42. Constr Build Mater 25(3):1236–1242

Ferro GA, Restuccia L (2016) Promising low cost carbon-based materials to improve strength and toughness in cement composites. Constr Build Mater 126:1034–1043

Geng G, Myers RJ, Qomi MJA, Monteiro PJM (2017) Densification of the interlayer spacing governs the nano-mechanical properties of calcium-silicate-hydrate. Sci Rep 7:10986

Gupta S (2021) Carbon sequestration in cementitious matrix containing pyrogenic carbon from waste biomass: a comparison of external and internal carbonation approach. J Build Eng 43:102910

Gupta S, Kua HW (2017) Factors determining the potential of biochar as a carbon capturing and sequestering construction material: critical review. J Mater Civ Eng 29(9):04017086
Gupta S, Kua HW (2018) Effect of water entrainment by pre-soaked biochar particles on strength and permeability of cement mortar. Constr Build Mater 159:107–125
Gupta S, Kua HW (2019) Carbonaceous micro-filler for cement: effect of particle size and dosage of biochar on fresh and hardened properties of cement mortar. Sci Total Environ 662:952–962
Gupta S, Kua HW (2020) Combination of biochar and silica fume as partial cement replacement in mortar: Performance evaluation under normal and elevated temperature. Waste Biomass Valorization 11(6):2807–2824
Gupta S, Kua HW, Tan CSY (2017) Use of biochar-coated polypropylene fibers for carbon sequestration and physical improvement of mortar. Cement Concr Compos 83:171–187
Gupta S, Kua HW, Low CY (2018a) Use of biochar as carbon sequestering additive in cement mortar. Cement Concr Compos 87:110–129
Gupta S, Kua HW, Koh HJ (2018b) Application of biochar from food and wood waste as green admixture for cement mortar. Sci Total Environ 619:419–435
Gupta S, Kua HW, Pang SD (2018c) Biochar-mortar composite: manufacturing, evaluation of physical properties and economic viability. Constr Build Mater 167:874–889
Gupta S, Kua HW, Pang SD (2020) Effect of biochar on mechanical and permeability properties of concrete exposed to elevated temperature. Constr Build Mater 234:117338
Gupta S, Kashani A, Mahmood AH, Han T (2021) Carbon sequestration in cementitious composites using biochar and fly ash—effect on mechanical and durability properties. Constr Build Mater 291:123363
Im S, Jee H, Suh H, Kanematsu M, Morooka S, Choe H, Yuhei N, Machida A, Kim J, Lim S, Bae S (2023) Insights on the mechanical properties of hierarchical porous calcium–silicate–hydrate pastes according to the Ca/Si molar ratios using in-situ synchrotron x-ray scattering and nanoindentation test. Constr Build Mater 365:130034
Junior AN, Filho RDT, Fairbairn EDMR, Dweck J (2014) A study of the carbonation profile of cement pastes by thermogravimetry and its effect on the compressive strength. J Therm Anal Calorim 116:69–76
Kaliyavaradhan SK, Ling TC (2017) Potential of CO2 sequestration through construction and demolition (C&D) waste—an overview. J CO2 Util 20:234–242
Kashef-Haghighi S, Shao Y, Ghoshal S (2015) Mathematical modeling of CO_2 uptake by concrete during accelerated carbonation curing. Cem Concr Res 67:1–10
Kim MS, Kang SH, Hong SG, Moon JH (2019) Influence of effective water-to-cement ratios on internal damage and salt scaling of concrete with superabsorbent polymer. Materials 12(23):3863
Kua HW, Gupta S, Koh S (2020) Review of biochar as a sustainable mortar admixture and evaluation of its potential as coating for PVA fibers in mortar. In: Tagliaferro A, Rosso C, Giorcelli M (eds) Biochar—emerging applications. IOPScience
Lagerblad B (2005) Carbon dioxide uptake during concrete life cycle—state of the art, Swedish Cem Concr Res Inst
Li N, Farzadnia N, Shi C (2017) Microstructural changes in alkali-activated slag mortars induced by accelerated carbonation. Cem Concr Res 100:214–226
Li J, Yu Q, Huang H, Yin S (2019) Effects of Ca/Si ratio, aluminum and magnesium on the carbonation behavior of calcium silicate hydrate. Materials 12(8):1268
Li J, Zhang W, Monteiro PJ (2020) Structure and intrinsic mechanical properties of nanocrystalline calcium silicate hydrate. ACS Sustain Chem Eng 8(33):12453–12461
Lim T, Ellis BR, Skerlos SJ (2019) Mitigating CO_2 emissions of concrete manufacturing through CO_2-enabled binder reduction. Environ Res Lett 14(11):114014
Liu Z, Meng W (2021) Fundamental understanding of carbonation curing and durability of carbonation-cured cement-based composites: a review. J CO2 Util 44:101428
Liu M, Hong S, Wang Y, Zhang J, Hou D, Dong B (2021) Compositions and microstructures of hardened cement paste with carbonation curing and further water curing. Constr Build Mater 267:121724
Madzaki H, KarimGhani WAWA (2016) Carbon dioxide adsorption on sawdust biochar. Procedia Eng 148:718–725
Maljaee H, Madadi R, Paiva H, Tarelho L, Morais M, Ferreira VM (2021) Sustainable lightweight mortar using biochar as sand replacement. Eur J Environ Civil Eng 1–17
Manzano H, Dolado JS, Ayuela A (2009) Elastic properties of the main species present in Portland cement pastes. Acta Mater 57(5):1666–1674
Maries A (1985) The activation of Portland cement by carbon dioxide, Proceedings of Conf. in Cem Concr Sci
Matschei T, Lothenbach B, Glasser FP (2007) The role of calcium carbonate in cement hydration. Cement Concrete Res 37(4):551–558
Mrad R, Chehab G (2019) Mechanical and microstructure properties of biochar-based mortar: an internal curing agent for PCC. Sustainability 11(9):2491
Muthukrishnan S, Gupta S, Kua HW (2019) Application of rice husk biochar and thermally treated low silica rice husk ash to improve physical properties of cement mortar. Theoret Appl Fract Mech 104:102376
Papadakis VG (2000) Effect of supplementary cementing materials on concrete resistance against carbonation and chloride ingress. Cem Concr Res 30(2):291–299
Praneeth S, Saavedra L, Zeng M, Dubey BK, Sarmah AK (2021) Biochar admixtured lightweight, porous and tougher cement mortars: Mechanical, durability and micro computed tomography analysis. Sci Total Environ 750:142327
Pu Y, Li L, Wang Q, Shi X, Fu L, Zhang G, Luan C, Abomohra AE-F (2021) Accelerated carbonation treatment of recycled concrete aggregates using flue gas: a comparative study towards performance improvement. J CO2 Util 43:101362. https://doi.org/10.1016/j.jcou.2020.101362
Roberts KG, Gloy BA, Joseph S, Scott NR, Lehmann J (2010) Life cycle assessment of biochar systems: estimating the energetic, economic, and climate change potential. Environ Sci Technol 44(2):827–833
Rostami V, Shao Y, Boyd AJ, He Z (2012) Microstructure of cement paste subject to early carbonation curing. Cem Concr Res 42(1):186–193
Shao Y, Rostami V, He Z, Boyd AJ (2014) Accelerated carbonation of Portland limestone cement. J Mater Civ Eng 26(1):117–124
Suescum-Morales D, Kalinowska-Wichrowska K, Fernández JM, Jiménez JR (2021) Accelerated carbonation of fresh cement-based products containing recycled masonry aggregates for CO_2 sequestration. J CO2 Util 46:101461
Tan PY, Sia A (2009) Understanding the performance of plants on non-irrigated green roofs in Singapore using a biomass yield approach. Nat Singapore 2:149–153
Teir S, Eloneva S, Zevenhoven R (2005) Production of precipitated calcium carbonate from calcium silicates and carbon dioxide. Energy Convers Manage 46:2954–2979
Wang X, Guo MZ, Ling TC (2022) Review on CO_2 curing of non-hydraulic calcium silicates cements: mechanism, carbonation and performance. Cem Concr Compos 133:104641
Xu X, Kan Y, Zhao L, Cao X (2016) Chemical transformation of CO_2 during its capture by waste biomass derived biochars. Environ Pollut 213:533–540
Yang X, Wang XY (2021) Strength and durability improvements of biochar-blended mortar or paste using accelerated carbonation curing. J CO2 Util 54:101766
You K, Jeong H, Huang W (2014) Effects of accelerated carbonation on physical properties of mortar. J Asian Archit Build Eng 13(1):217–221
Zajac M, Irbe L, Bullerjahn F, Hilbig H, Haha MB (2022a) Mechanisms of carbonation hydration hardening in Portland cements. Cem Concr Res 152:106687
Zajac M, Skocek J, Ben Haha M, Deja J (2022b) CO_2 mineralization methods in cement and concrete industry. Energies 15(10):3597
Zhan BJ, Xuan DX, Poon CS, Shi CJ (2019) Mechanism for rapid hardening of cement pastes under coupled CO_2-water curing regime. Cement Concr Compos 97:78–88
Zhang S, Ghouleh Z, Liu J, Shao Y (2021) Converting ladle slag into high-strength cementing material by flue gas carbonation at different temperatures. Resour Conserv Recycl 174:105819. https://doi.org/10.1016/j.resconrec.2021.105819
Zhang D, Shao Y (2016) Early age carbonation curing for precast reinforced concretes. Const Build Mater 113:134–143
Zhao M (2012) Quantitative control of C_2S crystal transformation. Appl Mech Mater 121:311–315